Bioengineered Rat Kidney Tissue Model for Drug Toxicity Assessment

An Honors Thesis for the Department of Biomedical Engineering

Erika J. Parisi
Tufts University, 2012

ABSTRACT

Nephrotoxicity is induced by a variety of marketed pharmaceuticals, and kidney toxicity is one of the main reasons for failure in preclinical safety trials. The launch of a novel drug on the market has proven an extremely time-consuming and expensive endeavor; therefore, innovative pre-clinical assessment methods are urgently required in order to better screen for more promising candidates. The development of a novel technique for the construction of a sustainable 3D rat kidney model upon which to evaluate the nephrotoxic effects of select pharmaceuticals is reported. Normal rat kidney epithelial and fibroblast cells were cultured in extracellular matrix molecules in order to develop the organ model. The results supported co-culturing with fibroblasts and indicated the collagen-matrigel mixture mediated optimal morphogenesis for both cell types. Structural features of the tubule-like formations of the kidney tissue were validated based on the distribution of GGT-1, Aquaporin 2, and Cytokeratin 8,18,19. Additionally, MTT and LDH cytotoxicity assays demonstrated a severe effect on the NRK52E and 49F cells, especially at 10 uM and 100 uM concentrations.

ACKNOWLEDGEMENTS

Professor David Kaplan, Ph.D.
Thank you for being my advisor over the past four years and supporting me throughout my development as a researcher. From the very first day you handed me the pamphlet describing all the research projects happening in your lab group and simply told me to 'Pick one,' you have allowed me to make decisions in the lab and trusted me. This has given me confidence I could have never developed inside a classroom, and I thank you for that. Anytime you want to take out a boat to row into Boston just let me know, there will always be a place for your single in the Shoemaker Boathouse!

Theresa M. DesRochers, Ph.D.
Thank you for being my research advisor on this project. From the very beginning you have been there on a daily basis, answering my constant questions, teaching me techniques, and helping to develop me into the scientist I have become.

Aiai Ren
As another undergraduate researcher, you helped me throughout the summer seeding, cutting, and staining tissue. You assisted me in the cell culture portion of my project and offered her help throughout my research. For that peer support, I thank you.

Michael Lambert
Michael graciously helped me format my fluorescent images and taught me how to navigate ImageJ.

Professor Kelly McLaughlin, Ph.D.
Thank you for supporting me throughout this entire process and helping me prepare for my defense. Additionally, your earnest interest in my project has provided me with constant enthusiasm.

Table of Contents

Index of Tables and Figures

1. BACKGROUND

1.1 Renal Anatomy and Physiology

1.1.1 Renal Anatomy

As one of the most intricate and unique organs in the body, the kidney (Figure 1) serves many functions vital to the survival of the organism including the filtration and excretion of metabolic waste products such as urea and ammonium, the regulation of necessary electrolytes, acid-base balance, and fluid, and the initiation of red blood cell production. Additionally, they reabsorb the essential nutrients such as glucose and amino acids, possess hormonal functionality through the stimulation of Vitamin D, erythropoietin, and calcitriol release, and control blood pressure by regulating the reabsorption of water (Ross, Romrell, and Kaye, 1995).

The surface of the kidney is surrounded by a thin but durable connective tissue capsule, consisting of an outer layer of collagen fibers and fibroblasts and an inner layer of myofibroblasts (Ross *et al.,* 1995). The inner portion of the kidney is divided into three sections—the renal cortex, the renal medulla, and the renal pelvis. On the outermost portion of the kidney, the renal cortex surrounds the organ. The cortex is characterized primarily by the renal corpuscles and their tubules. Renal corpuscles are the spherical structures that make up the beginning of the nephron segment and contain a unique collection of capillaries called the glomerulus (Ross *et al.,* 1995). The renal pelvis acts as a funnel to direct the urine produced by the kidney into the ureter for excretion from the organism. The renal medulla, the innermost section of the kidney, is the most relevant portion for my project. The medulla is subdivided into sections called renal pyramids, each containing straight, parallel nephron segments, which maintain appropriate levels of salt and water balance via the countercurrent exchange mechanism.

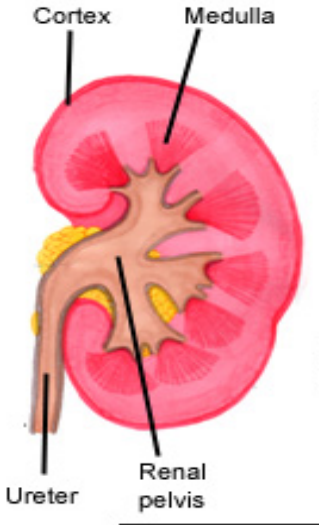

Figure 1. Anatomy of the renal system (Hoenig, Cheuck, and Gest, 2011)

1.1.2 Renal Physiology

The nephron, which is characterized by its unique segmental organization, is the primary functional unit of the kidney. Each nephron consists of a glomerulus, surrounded by the Bowman's capsule, proximal convoluted tubule, descending limb, loop of Henle, ascending limb, and distal convoluted tubule. Additionally, each nephron has an associated collecting tubule, which reabsorbs water before the filtrate is released into the ureter.

Consisting of a tuft of capillaries condensed into a small sphere, the glomerulus acts as the primary filtration mechanistic tissue. These filtering units of the kidney are formed by large, flattened segments of endothelial cells that are connected by thin diaphragms (Sands and Verlander, 2010). Underneath this layer lies the glomerular basement membrane, which has an associated negative charge. On the other side of this membrane are the glomerular epithelial cells. Filtrate entering the nephron must pass through all three layers, thereby the glomerulus structure significantly influences what molecules are permitted to pass into the nephron (Sands and Verlander, 2010).

Typically, larger proteins like albumin and hemoglobin are not permeable and, therefore, re-circulate into the bloodstream, whereas smaller molecules such as sodium and potassium ions or water easily pass through the pores (Ross *et al.,* 1995). The glomerulus receives about 20-25% of the cardiac output via the afferent arteriole before passing the filtrate through a double-layered epithelial cup to the capillaries of Bowman's capsule, from where it enters the proximal convoluted tubule.

The proximal thick segment, lined by cuboidal epithelial cells, is the primary site of reabsorption. Originating from the parietal epithelial layer of Bowman's capsule, the proximal tubule is subdivided into three segments—the S1 and S2, which represent the proximal convoluted tubule, and the S3, the proximal straight tubule. The S1 segment contains cells with a brush border as well as an extensive vacuolar lysosome and mitochondria due to the amount of active transport that occurs at this site (Sands and Verlander, 2010). While the transition from the S1 to S2 segment is gradual, there are distinct differences in the quantity and size of lysosomes. While the S3 segment has lower cell complexity than the S1 and S2 segments, the S3 is considerably more susceptible to injury due to the metabolic activation, hypoxia/reperfusion, or transporter-associated accumulation (Khan and Alden, 2002). This increases sensitivity in the S3 segment may be due to the decreased expression of cystolic NADP+-dependent isocitrate dehydrogenase (IDPc). IDPc synthesizes reduced NADP (NADPH), an essential cofactor for the generation of reduced glutathione (GSH), the most abundant and important antioxidant in mammalian cells (Kim *et al.,* 2009).

After receiving the filtrate from Bowman's capsule, the proximal tubule is responsible for actively reabsorbing glucose, sodium, and amino acids back into the bloodstream. In total, the proximal convoluted tubule reabsorbs about 80% of the primary filtrate (Ross *et al*., 1995).

Because the proximal tubule is highly permeable to water, as sodium is reabsorbed against its electrochemical gradient through the Na^+-K^-/ATPase pump located in the plasma membrane of the lateral folds, water passively flows through aquaporin channels back into the systemic circulation system. In addition, the proximal tubule regulates the concentrations of ammonia, chlorine, potassium, and hydrogen ions, as well as bicarbonate (Figure 2).

Because the cells of the descending limb are not specialized for reabsorption, the filtrate is only further concentrated by passing through a progressive gradient. This allows water to diffuse out of the nephron and back into the bloodstream. Once the filtrate has passed through the loop of Henle, it flows into the ascending limb of the nephron, which is impermeable to water. However, this segment is highly permeable to ions such as Na^+, Cl^-, and K^+, which travel out of the nephron and into the medullary interstitium by means of the Na^+-K^+/ATPase pump (Ross *et al*., 1995).

The distal tubule is the site of further filtrate concentration regulation. Specifically, NaCl tends to be actively reabsorbed into systemic circulation by means of the NaCl (NCC) co-transporter as well as the Epithelial Na^+ Channel (ENaC) (Ross *et al*., 1995). Additionally this segment is responsible for the continual reabsorption of the bicarbonate ion along with secretion of the hydrogen ion, creating a more acidic urine output. Lastly, the distal tubule is also the site of the conversion of ammonia into the ammonium ion, so that the body can excrete it, thereby avoiding the harmful effects of the toxic compound (Ross *et al*., 1995). The hormone aldosterone, released by the adrenal gland after stimulation by angiotensin II, acts to conserve sodium, while stimulating potassium release, thereby increasing water retention along with blood pressure of the organism.

The collecting duct is the site of final urine concentration and volume regulation. The regulatory hormone, antidiuretic hormone (ADH), secreted by posterior pituitary gland, acts to induce the translocation of the aquaporin channels of the nephron's plasma membrane, thereby increasing the permeability of the collecting duct.

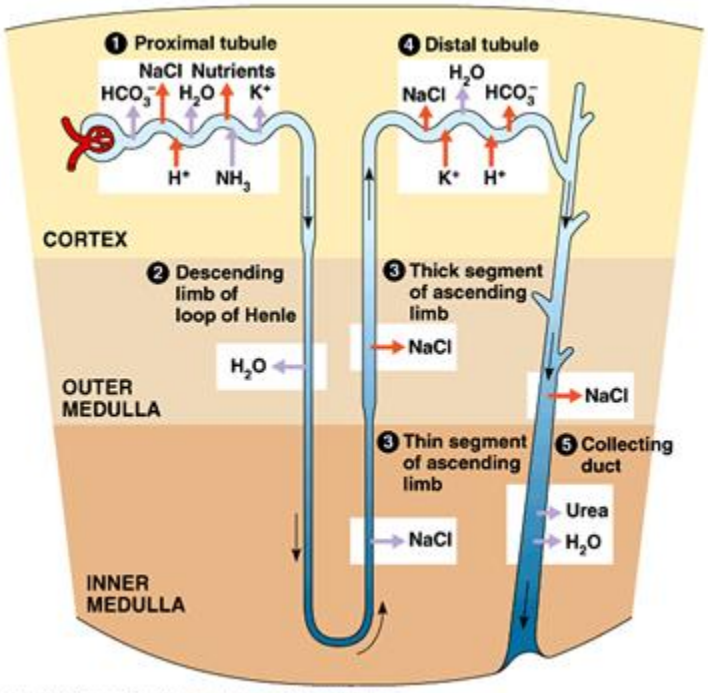

Figure 2. Schematic of a single nephron demonstrating the patterns of urine concentration and formation (Stanfield *et al*., 2008)

1.1.3 Origin of the Kidneys

A distinctive feature of the mammalian kidney is its development through three successive and unique phases, each resulting in a structurally more complex organ. These successive kidneys mature in a cranial to caudal orientation derived from the mesodermal cells of the intermediate mesoderm (Davidson, 2009). The subsequent order of maturation in amniotes such as mammals, birds, and reptiles is pronephros, mesonephros, and finally metanephros. The

pronephros and mesonephros, although functional in fish and amphibians, typically degrade *in utero* in amniotes, resulting in the formation of millions of nephrons as well as a highly elaborate branched collecting duct system characteristic of the metanephros as the definitive adult kidney (Davidson, 2009). However, these structures are necessary precursors for a metanephros.

1.2 FDA General Pathway for Novel Drugs

In order to introduce a novel drug into the public pharmaceutical market, it must undergo multiple extensive trials to prove that it is a safe as well as effective treatment option. The development of a new drug from the laboratory to the market is an incredibly time-consuming and expensive process, on average taking anywhere from 10 to 20 years and costing between 800 million and 1.7 billion dollars for each new compound (Pampalone, Stelzer, and Masotti, 2009).

Moreover, the failure rate of these novel drugs is astounding. A previous study has shown that around 92% of all proposed drugs fail sometime between the preclinical and clinical developmental phases (Knight, 2007); thereby calling for a more efficient pre-clinical method for drug-screening assay, improving upon the current standards (Figure 3).

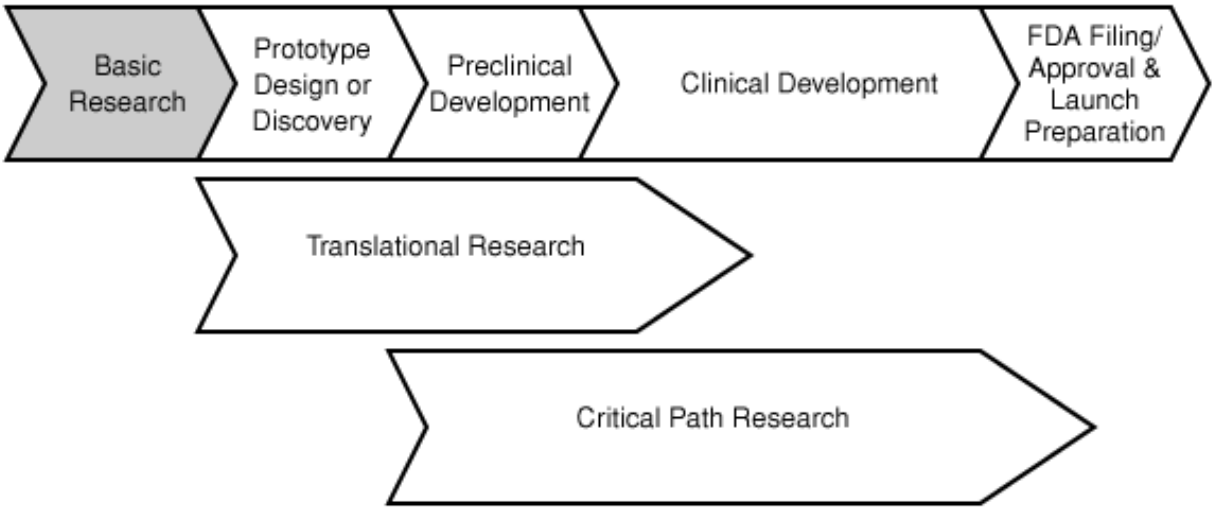

Figure 3. FDA Timeline. This image demonstrates the idealized path of a novel drug from the inception of the idea emerging from the scientific research to the approval into the public arena. The generated ideas enter an evaluation process before proceeding through the preclinical and clinical development. Only about 8% of all novel drugs become FDA approved and launched into the public sector (FDA: Challenges and Opportunities Report, 2004)

Basic research is aimed at identifying the background biological, chemical, and systemic processes of a certain disease. Scientific research eventually leads to the development of an idea, which is further cultivated during the translational research segment of the overall process. This section, including the design and development of a prototype, the pre-clinical studies, and a majority of the clinical developmental studies, is primarily designed to accelerate the conceptual framework of these ideas towards a relevant clinical, often therapeutic, implementation (FDA: Challenges and Opportunities Report, 2004). The Clinical Path Research, including the pre-clinical and clinical development as well as the final FDA approval, is concerned with establishing novel evaluation mechanisms in hopes of improving the product development process (FDA: Challenges and Opportunities Report, 2004).

1.2.1 Pre-Clinical Developmental Process Objectives

The design and development of a prototype phase is mainly concerned with material selection, structure, activity, and relationship to the desired outcome. While the clinical trials

deal with larger animal and human testing, the pre-clinical trials, those most relevant to my project, are focused on *in vitro* and smaller animal testing. These early trials assess the safety of the product, by proving the experimental drug is safe for primary human testing, as well as demonstrating medical utility, by selecting the most appropriate parameters for the highest probability of success in human trials. Pre-clinical trials for novel drugs typically undergo pharmacodynamics, pharmokinetics, absorption, distribution, metabolism, and excretion (ADME), and toxicity testing in order to determine its pharmacological activity (Pampaloni *et al*., 2009). Pre-clinical trials are a multi-faceted aspect of the path every novel drug must take in order to be implemented in the market and can be further subdivided into two types of screenings—primary and secondary.

1.2.2 Primary Screening Process

A primary screening is usually conducted in the laboratory on cells cultured in a 2D environment (Wilkinson, 2009). This process of screening has proven to be extremely inefficient because these conventional 2D environments fail to accurately mimic projected physiological responses to the experimental drug (Pampaloni *et al*., 2009). Moreover, the models are unable to serve as suitable models for later stages of drug evaluation trials; therefore, a secondary screening process must be carried out on smaller animals, including rats, mice, and rabbits. For these reasons, 3D culture environments are preferred in order to more accurately predict the effect of the drug *in vivo* (Table 1).

	2D Culture	3D Culture
Cell Shape	Flat; typical thickness of 3μm	Ellipsoidal; dimensions of 10-30μm
Architecture	Not physiological; cells partially interact	"Physiological"; promotes close interactions between cells; ECM growth factors
Cells Encapsulation	No	Yes
Growth Factor Diffusion	Rapid	Slow; biochemical gradients regulate cell-cell communication and signaling

Table 1. 2D v. 3D Culture. Adapted from (Kosovsky, 2011)

3D tissue models have been shown to allow for the use of biochemical, cellular, and molecular biology techniques to better understand the mechanism of toxic effects on tissue (Blaauboer, 2002). Recent advancements have focused on developing *in vitro* tissue models to assess the effects of respiratory-, neurological-, renal-, and cardio-toxicity (Blaauboer, 2002). With these novel paradigms, integrated, functional, multicellular systems can effectively mimic tissues and organs *in vivo*.

1.2.3 Secondary Screening Process

The secondary screening has also proven to be an ineffective system to predict success in human clinical trials. Recent drug screening data shows only 43% of the results seen using rodents were also expressed in the paired human clinical trial (Knight, 2007). In fact, a growing trend has been produced in the pre-clinical screening process that demonstrates these animal models are inefficient, as they are slower and more expensive than the comparable *in vitro* testing alternatives.

The secondary screening process typically involves dosing a lab rodent with an experimental drug to determine potential toxic effects as well as its safety at certain doses. Up until recently, most of these studies have focused on the effect of the drug on the body system;

however, studies are now shifting their concentration to determining the effect of the body system on the drug, such as how quickly it is metabolized once introduced.

Another difficulty researchers have faced with these secondary screenings has been dealing with animal rights activists as well as anti-vivisectionists organizations. These groups believe that any and all experimentation using animals is inherently wrong and unnecessary, and therefore, any kind of negotiation to reach a compromise has been impossible (Russel and Burch, 1992).

1.3 Nephrotoxicity

Nephrotoxicty is the poisonous side effects of harmful substances on the kidneys. When an organism is exposed to toxic materials such as chemicals or drugs, the effects may be dispersed equally throughout the system or may be manifested in a particular organ, termed the target organ of toxicity. With this in mind, scientists have come to study the effect of toxicants by means of their target organ. There are a number of factors including the pharmacokinetics of the compound, the metabolic fate of the compound, and the target organ's ability to respond to the toxic insult, that regulate how susceptible a specific organ is to toxicity (Pfaller and Gstraunthaler, 1998).

The three most studied organ tissues for toxicity are the heart, liver, and kidney. Due to the vital filtration function of the renal system, it is very important to monitor the effects of trial pharmaceuticals on the interconnecting systems of the body. The kidney specifically can exhibit an extreme manifestation of the toxic effects of a certain compound because of its inherent function. Because of its inherent dynamic nature, the kidney's renal structure and functions make it very susceptible to toxic substances. With its elevated rate of blood perfusion, intricate ion and

solute transportation systems, and its unique ability to recover water and thereby concentrate the solutes in the urine, the kidney is one of the most vulnerable organs to induced-cytotoxicity (Pfaller and Gstraunthaler, 1998).

Nephrotoxicity is diagnosed in the clinical setting by detecting a rise in the blood urea nitrogen (BUN) coupled with an increase in creatinine levels. The BUN levels reflect the amount of nitrogen present in the form of urea. An elevation of the normal range (in rat: 10-21 mg/mL) would indicate an excess of nitrogenous waste product, a condition that could manifest in a disease called uremia. Additionally, abnormally high serum creatinine levels would indicate the inability of the kidney to properly filter out the large amounts of serum creatinine, a byproduct present after the daily chemical breakdown of creatine. If the kidneys are damaged, it will result in an increase of serum creatinine present; however, not until 50% of kidney function has been lost.

The abnormal elevation in BUN and creatinine levels may be the result of a plethora of different conditions including dehydration, blockage of blood flow to or from the kidney, nephritis, diabetes mellitus, or – most relevant to my project – drug toxicity. Cisplatin is one such chemotherapy drug, whose use has been severely limited due to is severe nephrotoxic effects, and it was the experimental drug tested in this project.

1.4 Cisplatin and Current Studies Regarding Cisplatin-Induced Cytotoxicity

Cisplatin (*cis*-Diammineplatinum(II) dichloride), a platinum inorganic complex, is an extremely effective and widely used drug in chemotherapy treatments of many solid cancers including sarcomas, carcinomas, lymphomas, and germ cell tumors. However, its use has been severely limited due to its extreme cytotoxic effects. The cytotoxicity of cisplatin, whose

molecular structure is shown in Figure 4, is thought to be a result of a number of contributing factors, including peroxidation of the cellular membrane, mitochondrial dysfunction, inhibition of protein synthesis, and DNA injury that inhibits replication (Tsuruya *et al*., 2003).

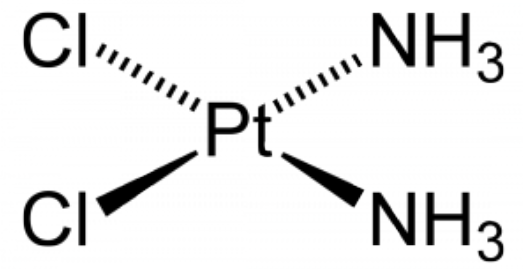

Figure 4. Molecular structure of cisplatin.

Yet, the most significant reason for cisplatin's limited use in cancer therapy remains its concentrated nephrotoxic effects, which have been linked to the highly reactive aquated metabolites formed. In fact, 20% of all patients receiving a high-dose cisplatin develop renal dysfunction (Yao *et al*., 2007). Nephrotoxicity due to cisplatin is determined primarily by reduced renal perfusion as well as an accumulating tubular defect (Arany and Safirstein, 2003).

1.4.1 Pathogenesis of Cisplatin

The effects induced by cisplatin occur primarily in the S3 segment of the proximal tubule, but also may be seen in the S1 and distal tubules of the nephron (Cristofori *et al*., 2007). The main effect of cisplatin on the S3 proximal tubular cells is necrosis or apoptosis, based on the severity of the injury. Cisplatin binds to nuclear DNA, by displacing one of the chlorine side groups with an aqua ligand. The aqua ligand can subsequently be displaced more easily, allowing for the platinum atom to bind to the nucleotide bases, especially guanine. This cisplatin-DNA crosslinking causes single and double-stranded breaks and thereby blocks further DNA synthesis and, as a result, gene replication. The damaged DNA produces repair signals. These signals may

include the production of DNA repair enzymes, or the delay of the cell-cycle progression. Ultimately, though, if repair is abandoned after failure, the signals will trigger cellular apoptosis (Jamieson and Lippard, 1999). Cisplatin also has been found to increase the intracellular levels of reactive oxygen species (ROS), which may be toxic to the internal organelles, thereby inducing damage to the cellular infrastructure leading to cell death (Sadzuka *et al*., 1994). ROS generated after an ischemia-induced renal impairment in cell proliferation and death performs a cell-type-specific, primarily in the tubular epithelial cells, and concentration-dependent role (Kim, Jung, and Park, 2010).

The disproportionate accumulation of cisplatin in the epithelial cells of the proximal tubule as compared to the extracellular serum has been thought to contribute to the nephrotoxic effects of the drug (Kuhlmann, Burkhardt, and Kohler, 1997). Cisplatin enters the cell via both transporter-mediated processes and passive diffusion, depending on the site of re-uptake. In the nephron, the most likely method of pathway of cisplatin is through transporter-mediated uptake (Kröning, Lichtenstein, and Nagami, 2000). In animals and humans, the most important cisplatin transporter in the proximal tubules is the organic cation transporter (OTC). This type of transportation is highly regulated and is polyspecific, electrogenic, voltage-dependent, pH-dependent, bi-directional, and Na^+ independent (Yao *et al*., 2007).

1.4.2 Cisplatin-Induced Nephrotoxicity Current Research

The specific cellular and molecular mechanisms causing the cisplatin-induced nephrotoxicity are not completely understood. Some past studies have observed that cisplatin may induce the activation of caspases, a family of cell death proteases, which play a significant role in apoptosis in renal tubular epithelial cells (Kaushal *et al*., 2001). A proposed pathway for

cisplatin-induced apoptosis is shown in Figure 5, in which the mechanism involves the subsequent activation of a number of caspases (Servais, *et al*., 2008). Additionally, high doses of cisplatin have been associated with specific gene changes. Specifically, there is an up-regulation of genes involved in drug resistance (MDR1, P-gp), cytoskeleton structure and function (*Vim, Tubb5, Tmsb10, Tmsb4x, Anxa2*), cell adhesion (*Spp1, Col1a1, Clu, Lgals3*), apoptosis (cytochrome c oxidase subunit I, BAR, heat-shock 70-like protein, Bax), tissue-remodeling (clusterin, IGFBP-1, TIMP-1), and detoxification (*Gstm2, Gstp2*) after cisplatin-induced injury.

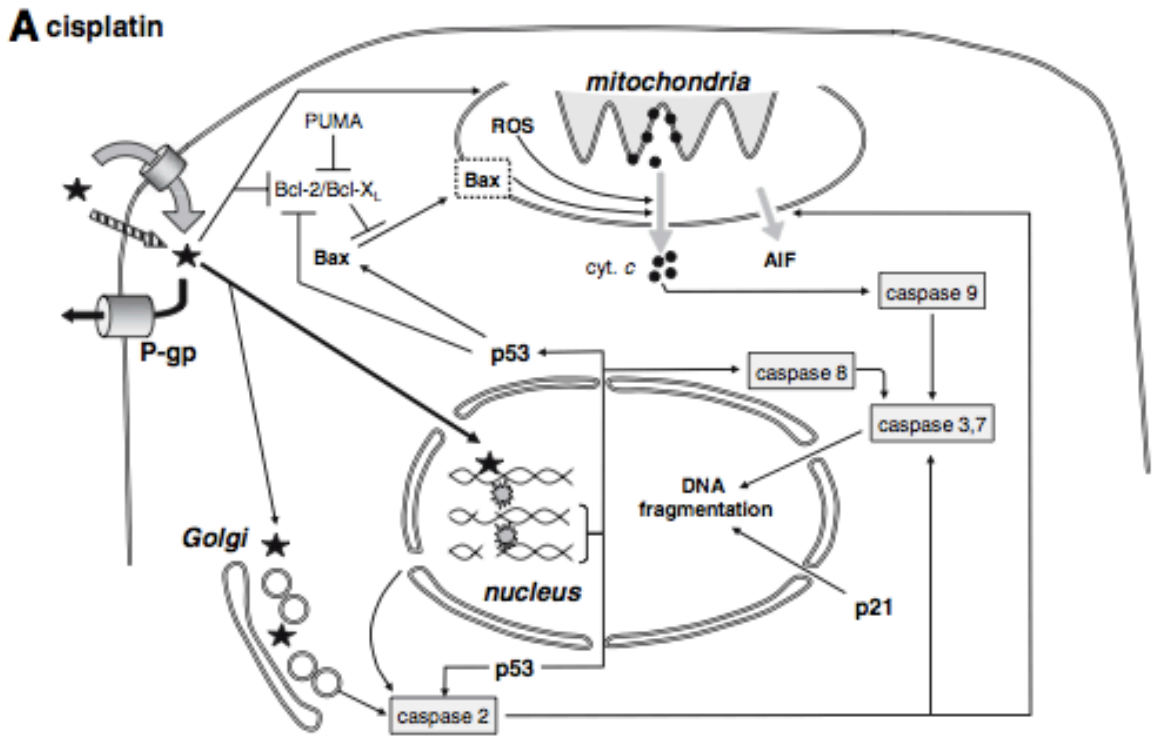

Figure 5. Mechanism for cisplatin-induced apoptosis. (Servais *et al.*, 2008)

Conversely, down-regulated genes include those centered near the proximal tubule (N-Acetyl-Beta-D-Glucosaminidase (NAG), *Odc1, Oat, G6pc, Kap*), those encoding gene factors and their binding proteins (*Egf, Ngfg, Igfbp3, Ghr*), and those controlling intracellular calcium homeostasis (SMP-30) (Huang *et al*., 2001, Leussink *et al*., 2003, and Thompson *et al*., 2004).

Once introduced into the body system, cisplatin induces a series of inflammatory responses, which play integral roles in the pathogenesis of the cisplatin-induced injury. Cisplatin also increases the expression of one major cytokine, tumor necrosis factor-α (TNF-α), which induces cellular apoptosis, produces reactive oxygen species, and coordinates the activation of a large network of chemokines and cytokines in the kidney (Ramesh and Reeves, 2002). Cisplatin has also been found to cause fibrosis surrounding the affected tubules along with infiltration of lymphocytes and macrophages. One study, conducted in live rats receiving 2mg/kg body weight cisplatin, found that the subjects developed fibrotic lesions in the corticomedullary junction (Yamate *et al*., 2002).

After 48 to 72 hours of a high-dose cisplatin administration, researchers have found significant impairment in the proximal and distal tubular reabsorption and increased resistance in the vasculature of a rat system. Cisplatin-induced toxicity has also been linked with decreased mitochondrieal ATPase activity, alteration of cell cation concentrations, and solute transport (Cornelison and Reed, 1993, Dos Santos *et al*., 2012). Additionally, the expression of water channels (aquaporin 1 and 2) in the outer medullary and sodium transporters (Na^+-K^+/ATPase α subunit, Na^+-K^+Cl^--cotransporter and Type III Na/H-exchanger), are diminished in rat models (Dos Santos *et al*., 2012, Lajer *et al*., 2005).

Cisplatin has therefore been linked to direct tubular injury via various mechanisms, but the effective contribution of each pathway is still unknown. Furthermore, current projects that

analyze the effect of cisplatin have yet to incorporate the 3D tissue engineering technique. Cisplatin is typically added to a 2D culture of rat kidney cells for an *in vitro* experiment or injected into a live animal model for an *in vivo* experiment.

2. INTRODUCTION

2.1 Clinical Significance

As one of the most integral organs in the body, the kidney, along with the liver and lung, has been considered the most important organs in determining targeted toxicity when a new drug or chemical is introduced into the body system. However, researchers are now finding that the kidneys may be even more susceptible than previously thought to toxic effects for a plethora of reasons.

While only accounting for a fractional percentage of the total body mass, the kidneys receive 20-25% of the cardiac output, guaranteeing that an appropriate level of xenobiotics are maintained in systemic circulation. Secondly, the kidney can concentrate tubular fluid, resulting in the unwanted effect of toxicity enhancement due to the elevated concentration of xenobiotics (Raju, Kavimani, and Uma, 2011). For these reasons, the kidneys are uniquely susceptible to introduced toxins and toxicants.

Revising the current method of animal testing has been a goal of scientific administrations for quite some time. The 3R-principle, which advocates the replacement of animal experiments, the reduction in the number of animals, and refinement of the stresses inflicted on the experimental animals, was developed by William Russel and Rex Burch (1959). Based on this philosophy, future methods of testing the toxicology of experimental drugs may evolve to avoid involving the use of live animal models. Therefore, a novel technique must be established and validated in experiments in order to achieve these advancements.

Animal testing, which is the most popular pre-clinical drug trial method, can be ethically controversial, expensive, and a poor predictor of drug response in humans. Rats metabolize drugs

differently than humans, thereby increasing the uncertainty of trial drugs in clinical trials; however, this 3D model will effectively bypass this issue, in that it is analyzing the effect of the drug directly on the kidney as opposed to taking into effect how it reacts with other physiological systems. Similarly, conventional 2D tissue models fail to accurately mimic responses to the drug *in vivo* (Pampaloni *et al*., 2009). In order to combat these limitations, 3D tissue cultures can be used to provide more accurate compound screening and can eliminate the toxic and ineffective substances at an early stage in the clinical drug trial process.

2.2 Specific Aims

The main aim of this project is to design a method for constructing a relevant 3D rat kidney model *in vitro* on which a certain antioneoplastic drug used for the treatment of solid tumors, cisplatin, can be tested in order to determine its nephrotoxic effects on the tissue. In order to successfully achieve this goal, two specific aims will be set.

2.2.1 Primary Specific Aim: Create a Relevant Tissue Model

The goal of the primary aim will be to create a relevant 3D rat kidney model *in vitro* that may be closely characterized with the native organ. In order to achieve this, the appropriate ratio of epithelial to fibroblast cell types must be attained. An optimal seeding density for the combination of normal rat kidney epithelial cells (NRK 52E) and normal rat kidney fibroblast cells (NRK 49F) will be identified and utilized for all tissue. It is known that the morphogenesis of epithelial cells is influenced by stromal interactions (Shimazu *et al*., 2001, Subramanian *et al*., 2010). The plasticity of the matrix molecules is also influenced by cells, including fibroblasts (Daley *et al*., 2008, Subramanian *et al*., 2010). For these reasons, it is necessary to include

fibroblasts in the 3D kidney tissue model. Furthermore, an appropriate ECM, consisting of relevant materials must also be used for the tissue construction process. Our working hypothesis is that a mixture of collagen type I, Matrigel™, and sodium hydroxide, will allow for the optimal environment. If the tissue product is deemed unsuccessful, we will vary the concentration of seeded cells, as well as the composition of ECM components. Additionally, Epidermal Growth Factor (EGF) will be added to the proliferation media in order to induce cell growth and proliferation in the tissue.

The outcome of this aim will be assessed using a Hemotoxylin and Eosin (H and E), Carmine-aluminum sulfate stain, and IHC stain for the expression of aquaporin II, γ-glutamyl transpeptidase, and cytokeratin 8,18,19. Table 2 describes the binding patterns associated with the stained proteins. These stains will allow for the assessment of cell density within the tissue as well as the patterns of organization. Ideally, cells will integrate into branching structures that resemble tubule formations.

Antigen Retrieval Protein	***Binding Patterns***
γ-Glutamyl Transpeptidase	Proximal Tubule Marker (IHC)
Aquaporin 2	Ductal Cell Marker (IHC)
Cytokeratin 8,18,19	Epithelial Cell Marker (IHC)

Table 2. Antigen retrieval proteins.

2.2.2 Secondary Aim: Assessing the Effects of Cisplatin on Healthy Kidney Model

The secondary aim will allow for the assessment of cisplatin on a healthy rat kidney cells, in both the 2D and 3D environments. The working hypothesis is that cisplatin will significantly reduce the amount of viable cells as well as diminish the quality of cell-cell interactions in the

tissue. This is caused primarily by the ability of cisplatin to initiate the breakdown of the cell membrane, thereby beginning the cellular degradation process and destroying the physical interactions between cells.

This aim will be assessed using a number of histological stains, including an H and E stain and Carmine-aluminum sulfate stain. Additionally, IHC analysis will be used to further characterize the effect of cisplatin on the tissue proteins associated with the nephron. To determine the cytotoxicity of cisplatin on cells the 2D environment, an MTT assay will be utilized. The MTT assay is a colorimetric assay to measure the viability of cells. This assay will assess the cytotoxicity of cisplatin on the NRK52E and NRK49F cells in a culture dish. The assay protocol involves converting the water-soluble MTT agent into an insoluble formazan. This formazan is solubilized, and its absorbance is measured to determine the amount of viable cells.

Lastly, to evaluate the cytotoxic effects of cisplatin on healthy kidney tissue in the 3D environment, an LDH (lactate dehydrogenase) assay will be conducted. The tissues, untreated with cisplatin, will serve as the control and a comparative standard for the other tissue. The LDH assay is used to quantify the amount of plasma membrane damage, which indicates cell death. LDH is present in most cells and is a stable, cytoplasmic enzyme. Upon damage to the cellular membrane, LDH is released from the cell into the culture supernatant. When the supernatant is collected, it can easily be assayed to determine the amount of cell death in a specific culture condition. A coupling reaction occurs that results in the oxidation of lactate by LDH to form pyruvic acid and NADH. NADH then reacts with diaphorase to produce the formazan. This red color absorbance is then measured at certain wavelengths to quantify the plasma membrane

damage. Below (Figure 6) is a simplified diagram of the principle behind the reaction that takes place in the LDH assay.

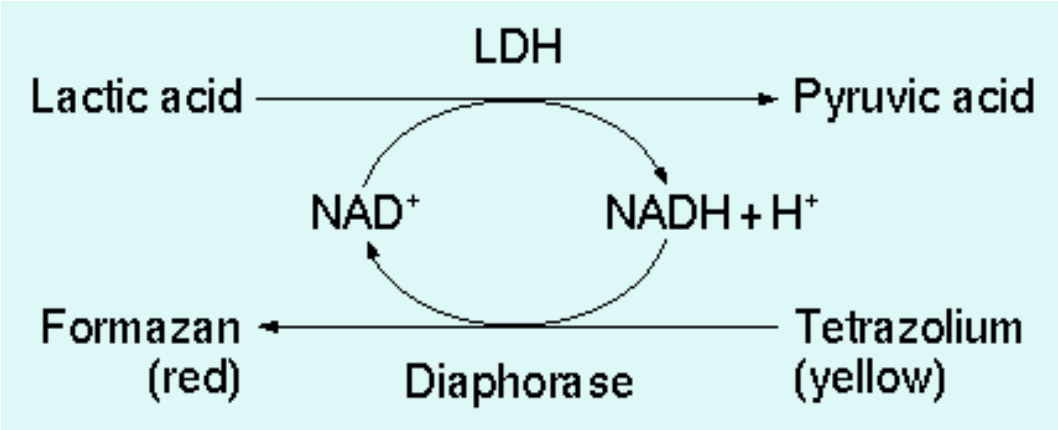

Figure 6. Principle of LDH assay measurement (TaKaRa Bio, 2012)

2.3 Long Term Goals

Ideally, this kidney model may be implemented into the FDA novel drug screening process as an additional check system before the drug is introduced into a live organism. By establishing this additional screening technique for novel drugs and pharmaceuticals, scientists may be able to reduce and refine the installment of the number of test organisms in the drug screening process. Furthermore, by implementing this tissue model into a perfusion bioreactor, researchers may be able to maintain tissue culture for an extended period of time so that a more accurate representation on *in vivo* conditions can provide information on the effects of cisplatin on the tissue. After this model has been effectively established using cisplatin as the test drug, the tissue may be utilized as a paradigm for different novel drugs in order to determine their nephrotoxicity before being placed into the live organism.

3. MATERIALS AND METHODS

3.1 Materials

NRK 52E and NRK 49F, both at Passage 0, were purchased from American Type Culture Collection (ATCC) (Rockville, MD). DMEM (Dulbecco's modified Eagle's medium), FBS (fetal bovine serum), 3-(4,5-dimethylthiazol-2-yl)-2,5-diphenyltetrazolium bromide (MTT) reagent, and penicillin-streptomycin (pen-strep) were purchased from Gibco (Invitrogen) (Eugene, OR). Epidermal Growth Factor (E. coli derived) (EGF) was purchased from R+D Systems (Minneapolis, MN). Growth Factor Reduced BD Matrigel™ Matrix and Rat Tail Collagen Type I (3.87 ug/mL) were purchased from BD Biosciences (Franklin Lakes, NJ). Cisplatin (cis-Diamineplatinum (II) dichloride) and Triton-100X were purchased from Sigma-Aldrich (Natick, MA). LDH Cytotoxicity Detection Kit was purchased from TaKaRa Bio (Shiga, Japan). Primary antibodies were purchased from Abcam (Grand Island, NY).

3.2 2D NRK 52E and 49F Cell Culture

3.2.1. Preparation of Proliferation Media

In order to ensure proper sterilization, all materials were pipetted into a 500 mL filter flask with a pore size of 0.2 um. 500 mL of Gibco® DMEM was added to the filter flask. It was then supplemented with 5% FBS and 1% Penicillin-Streptomycin. After the necessary components were added, the flask was attached to a vacuum, thereby activating the filtration mechanism. The resulting media was used for 2D cell expansion as well as tissue growth culture.

Before this media came in contact with the cultured cells or tissue, it was first warmed in a water bath kept at 37°C.

An additional media was used for culturing tissues and cells for the MTT assay. This media contained the same composition as the original; however, it was supplemented with EGF at a concentration of 0.02% of the total volume (100 uL EGF/ 500 mL media).

3.2.2 NRK 52E and 49F Cell Expansion and Passaging

Purchased normal rat kidney epithelial and fibroblast cells were thawed in a water bath at 37°C. In order to wash off the Dimethyl sulfoxide (DMSO), which had been added to the cells upon freezing, they were added to 8 mL of cell culture media. The resulting solution was centrifuged for 5 minutes at 1250 rpm at 25°C.

After the cell pellet had successfully been attained, the remaining DMSO and media were aspirated. The cells were then re-suspended with 5 mL of culture media. The 5 mL cell solution was then transferred to a T-185 tissue culture flask. An additional 20 mL of culture media was added to the flasks. Cells were incubated at 37°C in the presence of 5% CO_2. The cells were checked for confluence under a microscope 3 times per week, at which point the culture media was changed. Old media was aspirated and exchanged for 25 mL of fresh culture media. Media was added carefully to the sides of the flask, making sure not to shock the cells and thereby cause them to detach.

When the cells attained 80-90% confluency, they were passaged. Gibco® 0.25% Trypsin (1x) was thawed in a water bath at 37°C. While the Trypsin thawed, cells were washed with 15 mL of Phosphate Buffered Solution (PBS) to eliminate excess media from the flask. After the wash, the PBS was aspirated and 5 mL of warmed Trypsin was added to each flask. The flasks

were incubated at 37°C, 5% CO_2, for 5 minutes, providing ample time for the cells' attachment proteins to be degraded and allowing the cells to break free of the wall of the flask. After 5 minutes, the flasks were taken from the incubator and checked under the microscope to ensure adequate cell-detachment. 10 mL Culture media was then added to the flasks in order to stop the Trypsin reaction. The resulting solution was mixed and transferred to a 15 mL centrifuge tube. The solution was centrifuged for 10 minutes at 1250 rpm at 25°C. When the cell pellet had been attained, the remaining Trypsin and culture media was aspirated, and the cell pellet was re-suspended with 5 mL of fresh culture media. The cell suspension was thoroughly mixed, and 2 mL was added to a new T165 flask. 25 mL of fresh media was added. The cells were stored at 37°C, 5% CO_2.

3.3 3D Tissue Construction

A 12-well plate was used for the tissue construction process. First, the acellular layer, meant to provide a uniform extracellular environment for the engineered tissue, was created. For each well a total volume of 150 uL was added, consisting of 50% matrigel (75 uL per well), Collagen Type I (1 mg/mL), and 2M NaOH (0.023 M). The remaining volume was made up with PBS. After ensuring proper mixture of all three components by pipetting the solution up and down, 150 uL was added to each well. The plate was then incubated at 37°C, 5% CO_2 in order for the acellular layer to set, usually 30 minutes.

Meanwhile, the NRK 52E and 49F cells seeded in 165cm^2 flasks with a confluency of 80-90% were removed from the incubator to be trypsinized. The proliferation media was aspirated, and 10 mL of PBS was added to each flask in order to ensure all the media had been removed, so as to not interfere with the trypsin reaction. Cells were then trypsinized with 5 mL of Trypsin and

incubated at 37°C, 5% CO_2, for 5 minutes. After assuring the cells had become free-floating in the culture flask by examining them under the microscope, the reaction was stopped by adding 10 mL of warmed proliferation media to each flask. The proliferation media and trypsin solution were pipetted up and down in order to ensure cell detachment and reaction termination. This solution was added to a centrifugation conical and spun at 25°C at 1250 rpm for 5 minutes. After the pellet formed, the media and Trypsin solution was aspirated, and the cells were re-suspended in cellular proliferation media with EGF in a volume determined by the cellular layer remaining volume needed (see below).

The cellular layer was then created. For each well, a total volume of 400 uL of the cellular layer solution was added. This cellular suspension consisted of 50% matrigel (200 uL per well), Collagen Type I (1 mg/mL), and 2M NaOH (0.023 M). The remaining volume was made up with the NRK 52E and 49F cellular suspensions. The NRK 52E cell line was seeded at a density of 100,000 cells per tissue, and the NRK 49F were seeded at a density of 50,000 cells per tissue.

After the 400 uL of the cellular suspension was added to each well, the plate was incubated at 37°C, 5% CO_2 for 30 minutes in on order to ensure appropriate setting. After the incubation, 0.5 mL of proliferation media with EGF was added to the top of the tissue, and an additional 1.5 mL was added to the bottom of the well. See Figure 6 for detailed version of seeded tissue. Media supplemented with EGF was changed three times per week during the first two weeks of culture.

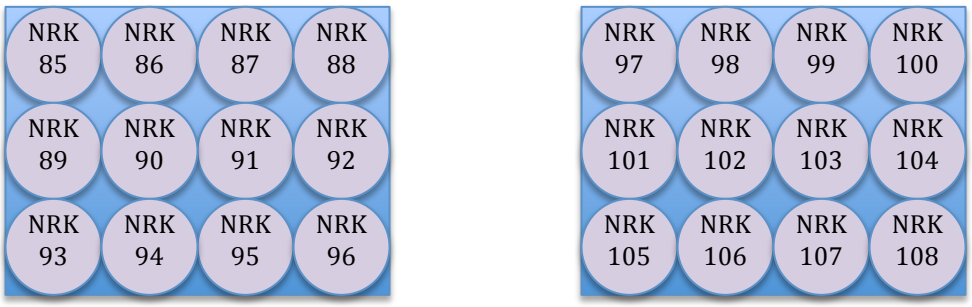

Figure 7. 3D Tissue construction in trans-well plates

3.4 Dosing with Cisplatin

After two weeks of culture, the tissues were dosed with cisplatin. Cisplatin was weighed and re-suspended to a final volume of 1 mM (5.14 mg/mL), which served as the stock for the sequential dilutions. The media in the bottom of each well (1.5 mL) was pipetted into separate, sterile, and labeled eppendorfs and placed in -80°C for future analysis (Figure 14). NRK 85, 89, and 93 were maintained in culture with normal EGF media thereby serving as the low control. NRK 86, 90, and 94 were introduced to EGF media supplemented with 1% Triton, serving as the high control. NRK 87, 91, and 95 were cultured with media with 0.01 uM cisplatin; NRK 88, 92, and 96 were cultured with media with 0.1 uM cisplatin; NRK 97, 101, and 105 were cultured with media with 1.0 uM cisplatin; NRK 98, 102, and 106 were cultured with media with 10 uM cisplatin; and NRK 99, 103, and 107 were cultured with media with 100 uM cisplatin. NRK 100, 104, and 108 were cultured with EGF-supplemented proliferation media and taken down (Figure 7) at the two-week point.

This dosing was repeated on Day 3 and Day 7 of the cisplatin incubation period. After three weeks of total culture time (1 week after initial cisplatin-exposure), the remaining tissues were taken down and fixed.

3.5 Carmine-Aluminum Sulfate Stain

Tissues were removed from the well using a scalpel cut in half, placed into a cassette, and stored in 10% buffered formalin at 4°C overnight. Half of the tissues were removed after 24 hours and washed with PBS for 10 minutes. This procedure was repeated before placing the samples in filtered Carmine solution (1g Carmine, 2.5g $KAl(SO_4)_2$, 500 mL dH_2O) overnight at room temperature. After 24 hours, the tissues were again washed twice for 10 minutes each in PBS and imaged using a Leica DMIL microscope.

3.6 Histology

Tissue samples were removed from the well using a scalpel cut in half, and placed into a cassette, stored in 10% buffered formalin at 4°C for 48 hours. Tissues were then processed, embedded into paraffin wax, and cut into horizontal cross sections using a Leica RM2255 microtome set to section in 8.0 uM increments. These sections were affixed to polarized slides and allowed to dry overnight on a warming plate set to 37°C. Histology samples were subjected to H and E staining and IHC for and γ-glutamyl-transpeptidase (GGT1), Cytokeratin 8,18,19 (CK8/18/19), and Aquaporin 2. Aquaporin 2 was probed with rabbit polyclonal (1:100) and goat polyclonal to rabbit IgG-Cy5 conjugate (1:200). GGT1 and CK8/18/19 were probed with mouse monoclonal (1:100) and goat polyclonal to mouse IgG-FITC conjugate (1:100). Bright field images of the H and E stained tissue samples were imaged using a Leica Fluorescence Microscope along with the Leica Application Suite software. A fluorescent imaging microscope Leica DMIL and black and white camera, Leica DFC340X, were used for the IHC sample imaging.

3.7 MTT Assay

An MTT assay was used to determine the cell viability of the NRK 52E and NRK 49F cells in culture with the EGF proliferation media after being dosed with cisplatin. NRK 52E and NRK 49F were trypsinized and re-suspended to a density of 50,000 cells/mL. From this suspension, 100 uL was added to a 96-well plate—48 of the wells were designated for the epithelial cell line whereas the other 48 wells were designated for the fibroblastic cell line (see Figure 8 for set-up)

24 hours after plating, the cells were exposed to 0, 0.01, 0.1, 1.0, 10, and 100 uM of cisplatin for 48 more hours. The solid cisplatin was suspended in proliferation media with EGF, and 100 uL of media with the desired concentration of cisplatin was added to the specific wells (Figure 8).

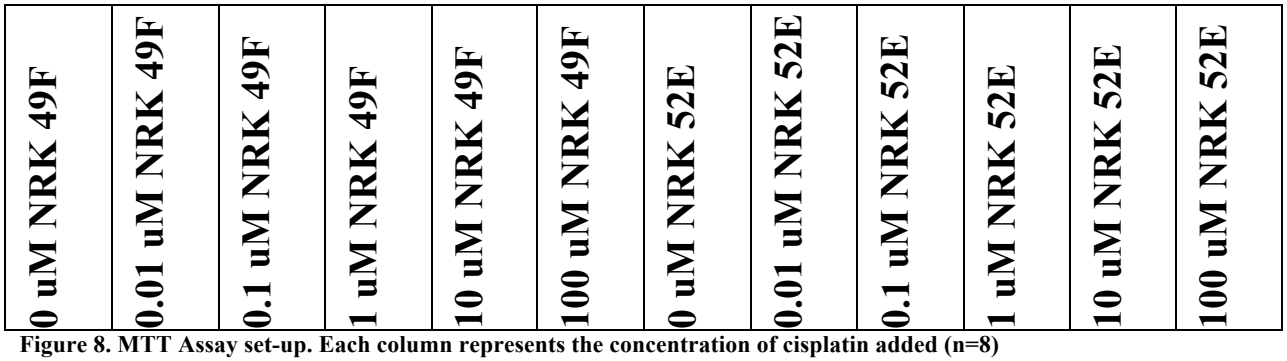

Figure 8. MTT Assay set-up. Each column represents the concentration of cisplatin added (n=8)

After the incubation with the cisplatin, 20 uL of MTT reagent dissolved in PBS (5 mg/mL) was added to each well and incubated at 37°C, 5% CO_2 for 5 hours. The media and MTT solution was then removed, and 100 uL of DMSO was added to lyse the cells. The cells were incubated in DMSO for 15 minutes at 37°C, 5% CO_2 for 15 minutes. The absorbance was read at 560 nm by a SpectraMax M2 (Molecular Devices).

3.8 LDH Assay

An LDH assay was used to evaluate cell death and cytotoxicity of the supernatant collected at specific time points (Day 0, 3, and 7) after the introduction of cisplatin into the media. The supernatant was removed from the -80°C freezer and allowed to thaw in the warm water bath for about 7 minutes. After it was thawed, 100 uL of supernatant was added to a designated well of a 96-well plate using a micropipette. LDH assay reagent (100 uL), created from the TaKaRa LDH Cytotoxicity Detection Kit, was then added to each well.

The plate was then wrapped in aluminum foil to block out any extraneous light and left at room temperature for 30 minutes. After 30 minutes, the plate was removed from the foil and the absorbance was read at 490 nm and 650 nm using the SpectraMax M2 (Molecular Devices). The % cytotoxicity was calculated as follows: (experimental-control)/(triton-control) x 100.

3.9 Statistical Analysis

MTT and LDH assay results were analyzed using PRISM software. Differences between culture media environments were determined by a two-way analysis of variance (ANOVA). A p-value ≤ 0.05 was considered significant and a p-value ≤ 0.001 was considered highly significant.

4. RESULTS

4.1 Proliferation Media

Tissues were found to develop tubular-like structures when cultured in media that had been supplemented with EGF as opposed to media without EGF (Figure 9).

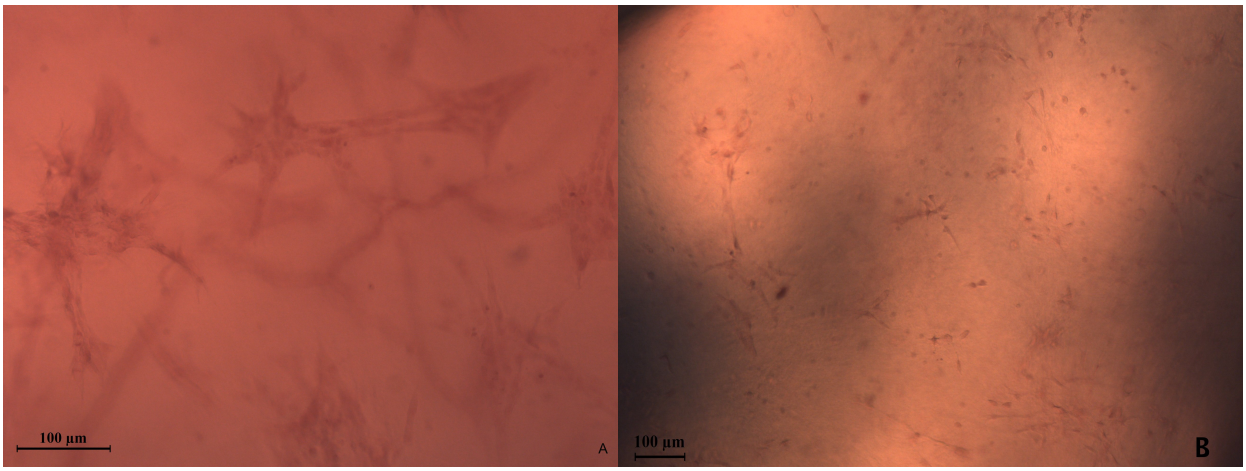

Figure 9. Carmine-aluminum sulfate stain for validation of proliferation media components. A) Tissues grown in the presence of media supplemented with EGF; B) in contrast, tissues grown in proliferation media without supplemented EGF.

4.2 Tissue Construction

Tissues grown with a mixture of 52E and 49F cells, seeded onto a silk scaffold within an ECM environment composed of matrigel and collagen, demonstrated cystic-like formations (Figure 10). Whereas tissues grown with only 52E or 49F demonstrated the cells' attraction to the scaffolding, thereby disallowing for any relevant structures to form. Taken together, these results suggested that a mixture of 52E and 49F cells is necessary to form a relevant kidney tissue model.

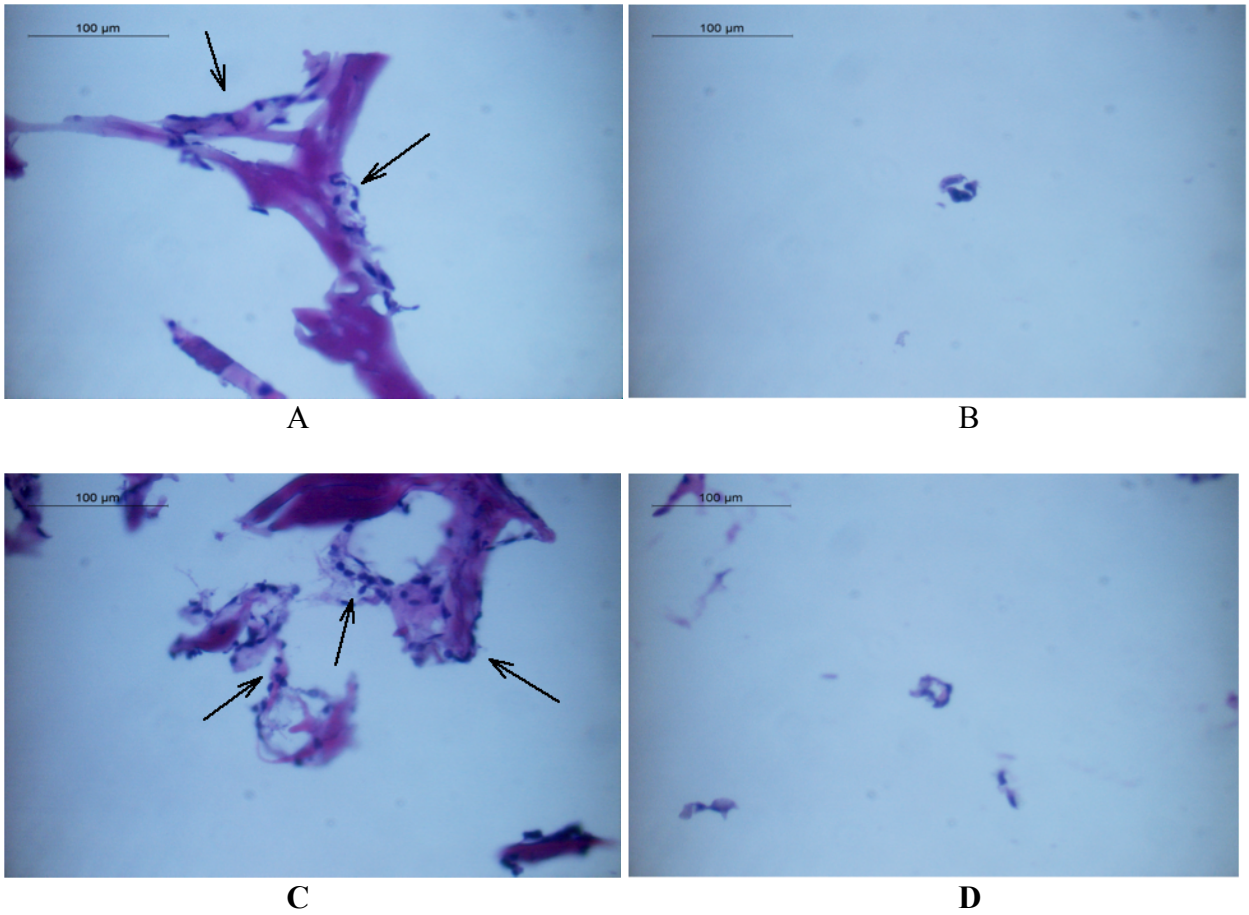

Figure 10. Engineered tissues with various cell mixtures. These images show that in A and C (NRK-49F and NRK-52E only cell-mixtures, respectfully), the cells are very attracted to the scaffolding (see arrows). However, in the B and D (combination of 52E and 49F 2:1, respectfully), some cystic-like structures have formed.

Before determining the ideal mixture of ECM components, a variety of different environments were used to grow tissue (Table 3). It was determined that a mixture of 50% matrigel (75 uL per well), Collagen Type I (1 mg/mL), and 2M NaOH (0.023 M) was optimal for tissue construction. The additional volume was made up of PBS. However, there were numerous other ECM environments and cell seeding types and densities that were tried before selecting the aforementioned description (Table 3).

Cell Types Seeded	ECM Contents	Comments
1. NRK-52E	a. Silk scaffold, 50/50 Matrigel, 1 ug/mL Collagen I, 2M NaOH	a. Cells were attracted to silk.
	b. Matrigel Only	b. Tissues lacked structural integrity. No structures formed.
2. NRK-49F	a. Silk scaffold, 50/50 Matrigel, 1 ug/mL Collagen I, 2M NaOH	a. Cells were attracted to silk.
	b. Matrigel Only	b. Tissues lacked structural integrity. No structures formed.
3. NRK-52E and NRK-49F	a. Silk scaffold, 50/50 Matrigel, 1 ug/mL Collagen I, 2M NaOH	a. Cells were attracted to silk.
	b. Matrigel only	b. Tissues lacked structural integrity. No structures formed.
	c. 1 ug/mL, 2ug/mL Collagen I, 50/50 Matrigel, 2M NaOH	c. No relevant structures formed. Cells were not organizing into tubes.
	d. 1 ug.mL Collagen I, 50/50 Matrigel, 2M NaOH, media +EGF	d. Selected environment.

Table 3. Summary of tissue construct attempts

After collecting data from the previous experiments, the tissue construction criteria with the most optimal tissue construct product were found to be those of condition 3d. All tissue dosed with cisplatin included these conditions. Additionally, tissues supplemented with 100,000 52E and 50,000 49F per well showed better branching structures (Figure 11).

4.3 Carmine-Aluminum Sulfate Stain

In order to determine the branching tubular nature of the formed tissue, the Carmine-aluminum sulfate stain was used. Shown below are the representative images (Figure 11) for the tissues. The degree of the epithelial branching structures may be used to determine the overall growth and viability of the tissue.

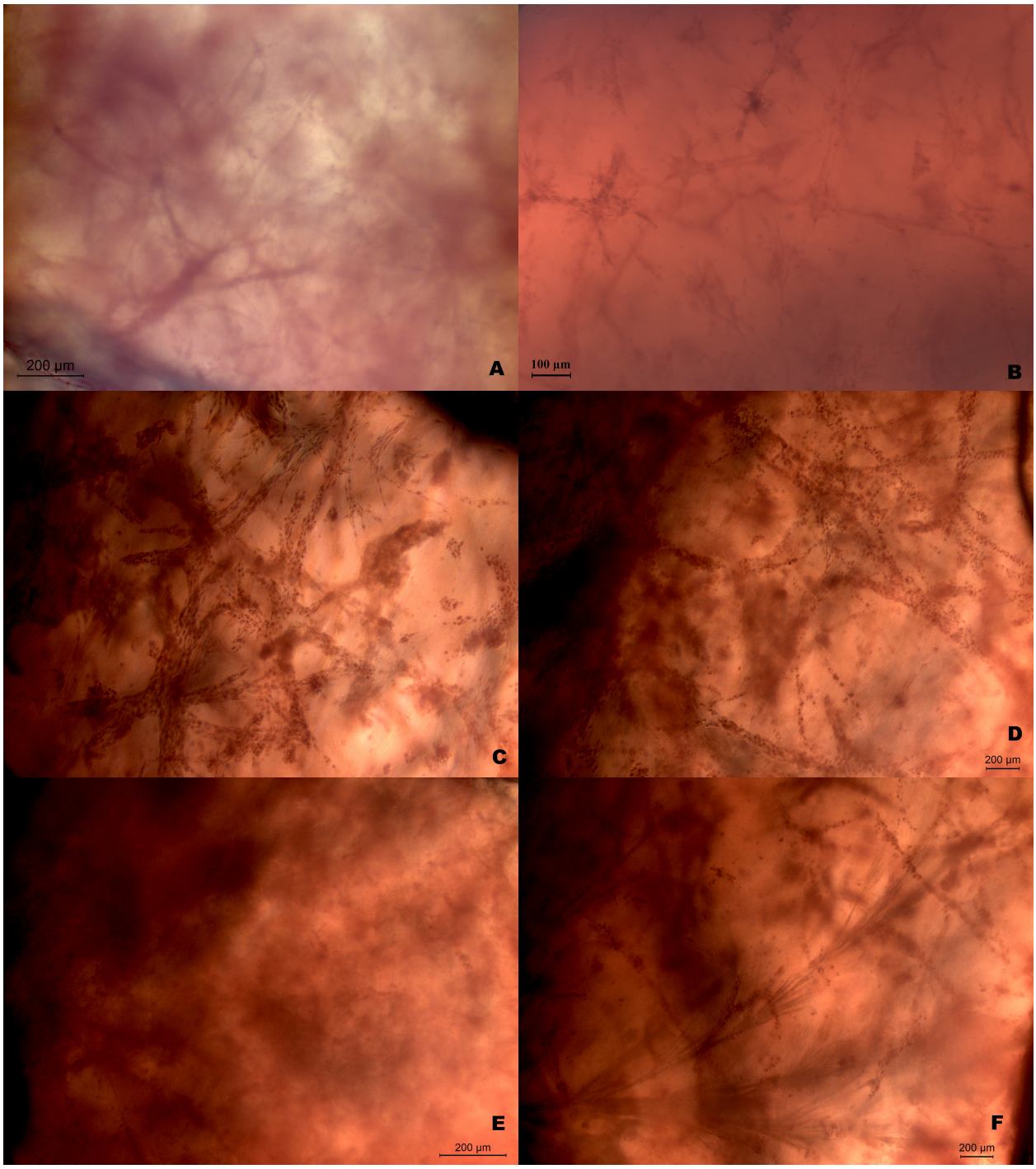
200 µm
A
100 µm
B
C
D
200 µm
E
200 µm
F
200 µm

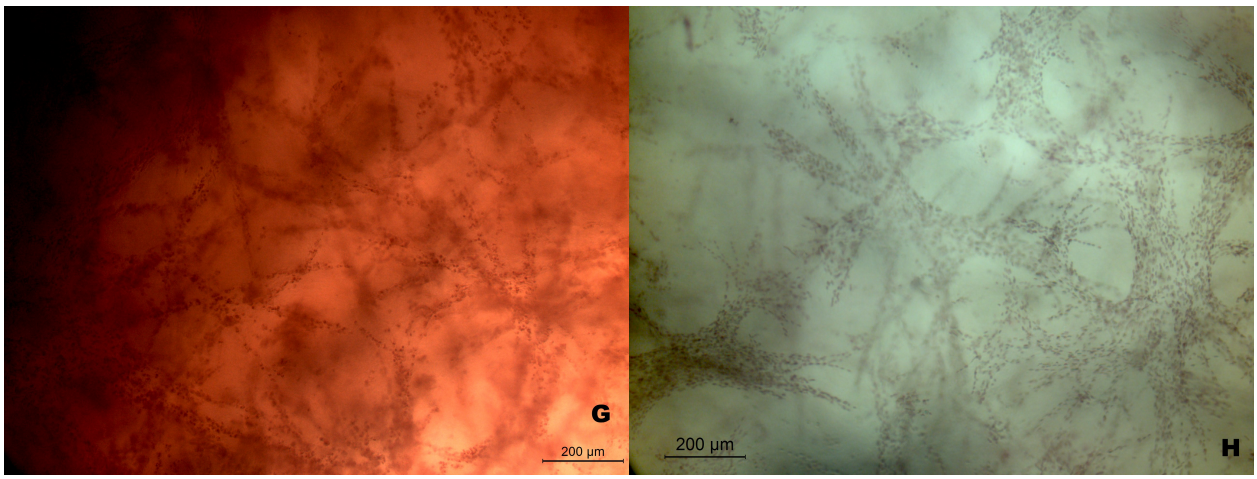

Figure 11. Representative carmine stain on tissues. A) Two-week tissue B) Four-week tissue C) 0.01 uM cisplatin (3-week) D) 0.1 uM cisplatin (3-week) E) 1.0 uM cisplatin (3-week) F) 10 uM cisplatin (3-week) G) 100 uM cisplatin (3-week) H) 1% Triton (2.5-week)

Tubule structure showed degradation in conditions with greater than 0.01 uM of cisplatin supplemented in the media, a concentration expected not to significantly impact the tubulogenesis of the 3D tissue. Figure 11h represents the high control. Tissues in this condition were exposed to proliferation media containing 1% Triton, in order to effectively kill all cells within the engineered structure. The breakdown of the plasma membrane, a result associated with cell apoptosis, is visible in Figure 11c-h.

4.4 Tissue Characterization Stains

The H and E stain (images not shown) demonstrated that the tissues exposed to all concentrations of cisplatin had large amounts of dead space, indicating cellular apoptosis. Cells appeared to be forming into tubules; however, the large empty spaces surrounding tubule-like structures indicated the cells had begun to die. There were significantly more areas of dead space in the tissue exposed to the higher doses of cisplatin, as compared with the untreated, but a cell death assay must be conducted in the future in order to confirm this claim.

The antigen retrieval stain was used in order to characterize the kidney model developed with this tissue engineering method. Because this stain was carried out only on healthy tissue, we

expected to see normal distribution of proteins along the cellular formations. The IHC staining was used to further characterize the tissue. Both the Aquaporin 2 and GGT1 stains showed positive results (Figure 12a,b). The positive Aquaporin 2 stain indicated ductal formations, while the positive GGT1 stain indicated the engineered proximal tubule. The CK8/18/19 stain had large amounts of non-specific background fluorescence. Dapi blue staining represented the cell nuclei.

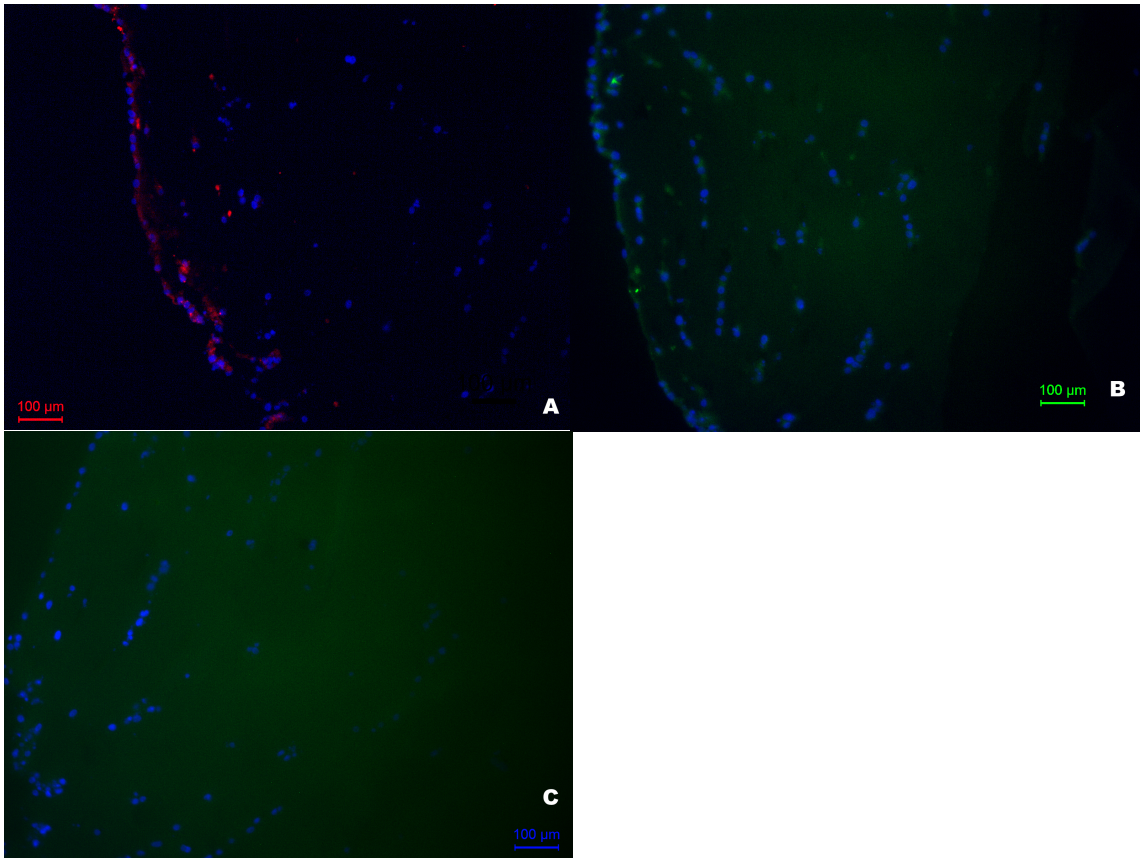

Figure 12. IHC Images. A) Dapi and Auaporin 2 B) Dapi and GGT1 C) Dapi and CK8/18/19

4.5 MTT Assay

The results of the MTT assay demonstrated a significant decrease in cell viability between both the normal condition and 10 uM as well as the normal and 100 uM conditions

(Figure 13). There was a greater effect in the decrease in viability in the epithelial cells as compared to the fibroblast cells.

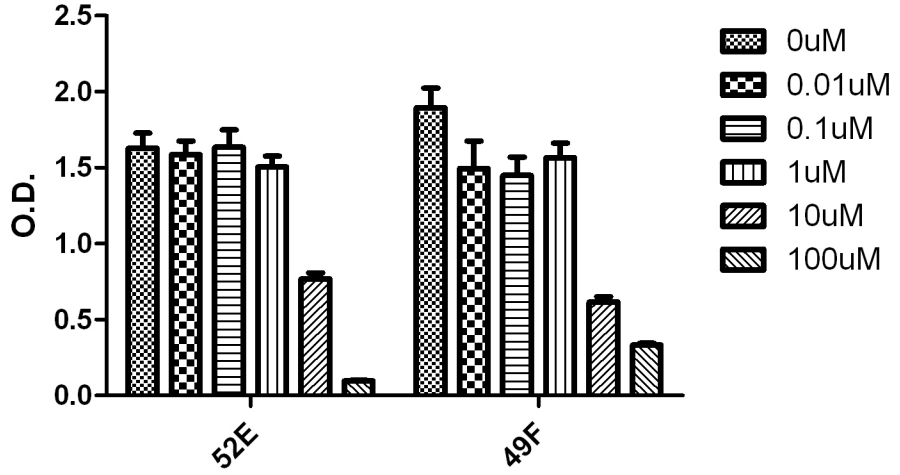

Figure 13. MTT assay results. Values represent the mean ± the SEM after the exposure of the NRK 52E and 49F cells to cisplatin-supplemented media at specific concentrations for 48 hours (n=8)

In the MTT assay, the OD decreased most significantly with the higher concentrations of cisplatin (10 uM and 100 uM) in both cell types. The p-values for the comparison of reductions between the untreated 52E and 49F cells to those exposed to 10uM and 100uM of cisplatin-supplemented media were both highly significant ($p<0.001$). These results compared well with previous studies (Rodriguez-Garcia *et al*., 2009, Sirichanchuen *et al*., 2012, Leibrandt *et al*., 1995). The 52E cells were more severely affected by the higher concentration of cisplatin. Comparing the control condition to the 10 uM condition, the results indicated a 67.7% decrease for 49F and a 52.8% decrease for 52E in cell viability. Furthermore, comparing the control condition to the 100 uM cisplatin concentration condition, we found an 82.5% decrease for the 49F and a 94.1% decrease for 52E in cell viability.

4.6 LDH Assay

The results of the LDH assay, Figure 14, demonstrated the highest percentage of cytotoxity was associated with the 100 uM cisplatin culture condition. However, the lower concentrations also exhibited a higher than anticipated percentage of cytotoxicity (Fukuishi and Gemba, 1989). No statistical significance was seen in any of the tissue other than the control to the 10 uM and 100 uM culture conditions on Day 3 of culture only ($p < 0.05$).

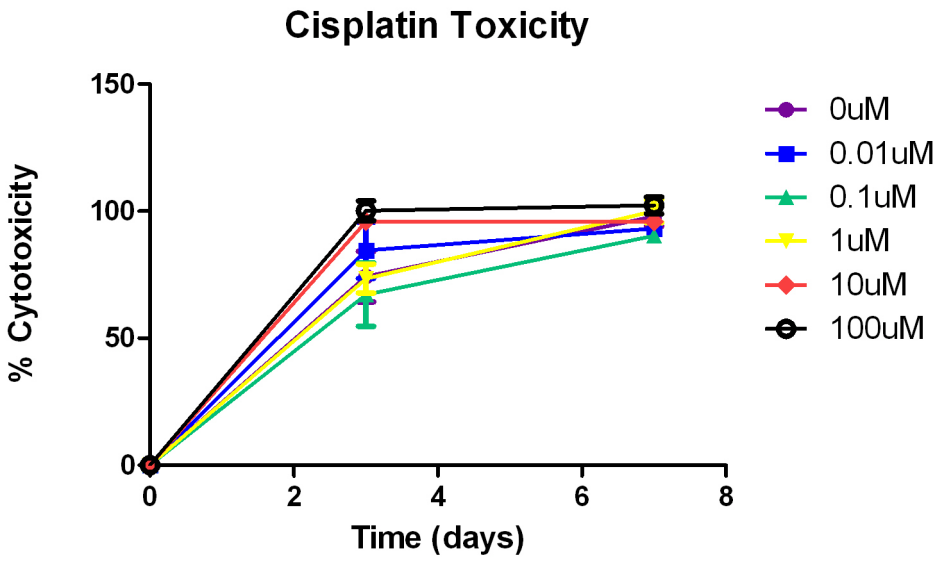

Figure 14. LDH assay results for rat kidney model. Values represent the mean ± the SEM. Supernatant samples were collected at Day 0, 3, and 7 after exposure of the tissue to cisplatin-supplemented media at specific concentrations (n=3).

5. Discussion

5.1 Tissue Construction

After conducting numerous tissue constructions, we had a clear idea about what cell densities should be seeded as well as the necessary ECM components to form a relevant kidney model. It was necessary to incorporate both fibroblasts and epithelial cells in order to develop the relevant 3D kidney model as was expected (Daley *et al*., 2008, Subramanian *et al*., 2010). Because the morphogenesis of epithelial cells is extremely responsive to degradation lifetimes, inflammatory hydrolytic degradation products, and issues of mechanical strength, the composition and state of ECM components had to be artfully deduced through a series of construction attempts. The components we included are known to be biocompatible and retain their properties to mediate the morphogenesis of NRK 52E and 49F cells (Subramanian *et al*., 2010).

Furthermore, research suggested that the addition of another growth factor, EGF, would promote the elongation of the developing kidney tissue, thus inducing the formation of tubule-like structures (Zhou *et al*., 2010). This finding was further supported in our research. Figure 9 demonstrated the tubulogenesis in tissue exposed to EGF-supplemented media; however, no tubule-like formations were seen in tissue grown in proliferation media without EGF. Therefore, it may be concluded that the addition of EGF is essential in inducing the NRK 52E and 49F cell mixture to develop single-cell branching morphogenesis and multicellular tubulogenesis. This may be linked to EGF's known ability to induce protein synthesis and proliferation in rat proximal tubule cells (Villegas *et al*., 2005).

These tissues were grown in a static culture for only four weeks. In order to increase the sustainability and allow for this technology to be implemented in pharmaceutical testing, a more workable model must be generated. This may include using some sort of scaffolding in order to lend more structure and stability to the growing tissue model. Additionally, the utilization of a perfusion bioreactor system that mimics *in vivo* conditions has been proven to increase the amount of efficient mass transfer as well as maintain the tissue culture for longer periods of time (> 8 weeks) (Subramanian *et al*., 2010). Lastly, because the H and E stains indicated large amounts of cell death, a TUNEL assay to measure the amount of cell death would likely yield informative results on the amount of DNA damage, resulting from apoptotic signaling cascades. Additionally, an LDH assay should be conducted during the initial culture period of the tissue before introducing cisplatin into the media in order to better assess the cytotoxicity levels of the developing product. Therefore, we may get a better idea of the state of the tissue before the introduction of cisplatin.

5.2 Tissue Characterization

5.2.1 IHC Staining

In order to determine whether the tissues formed were actually kidney specific rather than a random accumulation of the seeded cell types, IHC stains for GGT1, Aquaporin 2, and CK8/18/19 were conducted. The GGT1 and Aquaporin 2 antibodies demonstrated an appropriate distribution along the cellular formations. However, the CK8/18/19, which is the marker for epithelial cells, showed non-specific staining of the tissue. Although the green color was concentrated within the confines of the tissue, we cannot definitively say that these results indicated that we made epithelial cells. This non-specific stain could indicate that the cells found

in the tissue are not epithelial cells. Epithelial cells are the integral cell type for the nephron; thus, if our tissue does not exhibit this cell kind, it is necessary to reconstruct the model and perhaps alter the cell densities seeded. However, the stain does appear to have brighter green areas of fluorescence centralized along the tubular formations. This cytokeratin stain should be re-conducted, with careful consideration paid to the blocking step of the protocol.

The Aquaporin 2 and GGT1 stains indicated more promising tissue characterization. The GGT1 stain accumulated near the cell nuclei, indicating a positive result for proximal tubule formations. The Aquaporin 2 stain indicated a small number of cells testing positive for the collecting duct marker. These results allowed us to more definitively characterize the engineered tissue as kidney. Although other cell types may express some of these genes, future stains for more characteristic proteins such as E-cadherin, Collagen IV, and Aquaporin 1 may give a better representation of the tissue product formed.

Additional stains that should be conducted in the future may include E-cadherin, which would allow for better analysis of the epithelial cellular junction formation, and Collagen IV and Laminin, both of which indicate the polarity as well as the basement membrane (Subramanian *et al*., 2010). With these additional stains, we may be able to accurately showcase the unique distribution patterns characteristic of native kidney tissue.

Additionally, because tubules are the most desired structure of the kidney during the tissue engineering process, it is necessary to determine that the structures formed are, in fact, tubules rather than a simply the interactions of cellular projections. A recent study that involved the development of a 3D mouse kidney model demonstrated positive tubulogenesis by a series of IHC stains for biomarker proteins including E-cadherin, N-cadherin, and Na^{+}-K^{+}/ATPase pump

(Subramanian *et al.,* 2010). Using this positive result, we can expect eventually the same positive tubulogenesis formation in the rat model, allowing for a relevant model.

5.2.2 Carmine Staining

The data collected from the carmine stain help inform us on the level of tubulogenesis and connectivity among cells in growing kidney tissues. Although the untreated tissues (Figure 11a and b) demonstrate continuous tubule-like attachments throughout the model, tissues exposed to concentrations of cisplatin as low as 0.01 uM showcased signs of high cytotoxicity and tubule degradation. The breakdown of connection is visible in the individualization of cells within the tissue. Instead of a singular, continuous tubule formation, a series of smaller circular fragments may be seen in the tissue exposed to media supplemented with a specific dose of cisplatin. This is due primarily to the breakdown of the plasma membrane of the epithelial cells, an effect of cellular apoptosis, which occurs through the proteolysis of cytoskeletal and plasma membrane proteins (Liu *et al*., 2004).

While the initial hypothesis led us to believe more intense tubule degradation would only be visible at higher concentrations (>10 uM), the breakdown of intercellular connections at the lower cisplatin concentrations may be explained. Because the cells that were used had not formerly been established in a previously successful tissue construction, the cells may not have been as initially viable as the earlier cultures. Additionally, the static 3D environment may have contributed to the decline of structural soundness and cellular viability, due to the lack of efficient mass transfer (Subramanian *et al*., 2010). Therefore, when attempting to repeat this experiment, it will be necessary to use a cell line that has been successful in previous construction attempts as well as incorporate the system eventually into a perfused bioreactor design.

5.3 Cell Viability and Toxicity in 2D and 3D Environments

The MTT assay, which was used to understand how cisplatin affected the cell types in a 2D environment, showed that at higher concentrations (10 uM and 100 uM), cisplatin inhibits the viability of both NRK 52E and 49F. Additionally, Figure 13 indicated that the NRK 52E cells were more affected at the largest concentration of cisplatin (82.5% decrease in cell viability (49F) versus 94.1% decrease in cell viability (52E)).This may be due to the fact that epithelial cells have the associated megalin receptor, that allows for the receptor-mediated endocytosis of cisplatin (Riedemann *et al*., 2007). Megalin is an endocytotic receptor that is expressed in polarized cells such as those of the proximal tubular portion of the kidney. This receptor has been associated with the uptake of aminoglycosides, which are known, like cisplatin, for their nephrotoxic effects (Schmitz *et al*., 2002).

Because fibroblasts lack this megalin receptor, the cisplatin must rely on an alternative method to enter the 49F cells. Although the pathway of cisplatin into fibroblast cells is not well understood by researchers, an association has been found between the hyaluronan binding protein 1 (HABP1/p32/gC1gR), which is located on the cellular membrane, and is upregulated upon the induction of cisplatin into the cell media (Meenakshi *et al*., 2002). Furthermore, the upregulation of HAPB1 has been closely associated with the induction of cellular apoptosis (Guo *et al*., 1999).

The LDH assay, which was used to understand how cisplatin affected the cell types in a 3D environment, resulted in unexpected data. While the comparisons between the control and 10 uM and 100 uM conditions proved to be highly significant ($p<0.001$) on Day 3, there were no other statistical comparisons that could be confidently drawn with this data. The graph

demonstrated that all conditions exhibited high levels of cytotoxicity at the end of seven days of exposure of the tissue to cisplatin. Figure 15 below shows the results seen in a 3D *in vitro* human kidney model. In this figure, the tissues introduced to 100 uM of cisplatin shows the highest percentage of cytotoxicity, with those exposed to 10 uM of cisplatin following a similar curve, but with a slightly lower overall percentage. This graph indicates the type of result we expected to see with the rat model; however, our data may indicate a higher susceptibility of the NRK 52E and 49F cells to cisplatin-induced cytotoxic effects. Additionally, my project involved using immortalized cells, which are known to react differently to established toxicants.

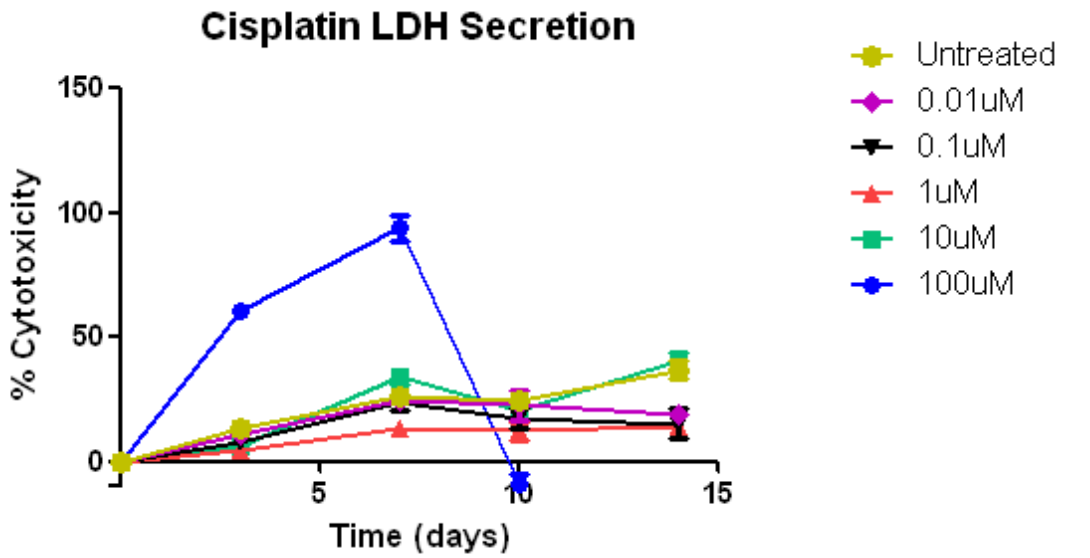

Figure 15. LDH Assay from Theresa M. DesRochers (Tufts University, 2011)

Our results may be indicative of the extremely high, and clinically limiting, cytotoxicity of cisplatin on kidney tissue. Although the lower concentrations have not been validated in previous experiments to cause as much cytotoxicity as was present in our data, the use of these tissue construction parameters (ECM components, cell seeding density, etc.) may have disallowed for as structurally sound a tissue model to develop. This would explain the dramatic decrease in cell viability at only high concentrations of cisplatin (>10 uM) in the 2D analysis,

opposed to the extremely high percentage of cytotoxicity in all concentrative doses in the 3D LDH assay.

However, there may be other reasons for this particular data result. These differences among 2D and 3D may be due to a number of reasons. The 3D tissues were left in the cisplatin-supplemented media for 7 days (336 hours); however, the cells used for the 2D MTT assay were only exposed to cisplatin for 48 hours before the absorbance was measured. The difference of 288 hours may have allowed for greater cytotoxic effects on the tissue model, thereby yielding a more severe damage to the tissue. Additionally, the tissue media in the trans-well plates was changed every 3-4 days. This extended exposure to older media could have induced premature cell death, even in the non-dosed tissue. If culture media is not changed frequently enough, nutrients may become depleted and metabolic products may increase in concentration, which may be toxic to cells. This could explain why the H and E stain demonstrate areas of dead space in tissue that should have exhibited healthy characteristics.

In order to better account for the influence of the older media on the overall viability of the tissue, future experiments should allow for tissue culture media to be changed more frequently (every 2 days). Additionally, the incorporation of this model into a perfusion bioreactor system would ensure that the tissue is constantly in contact with fresh proliferation media. This may better protect against the buildup of metabolic products and may result in a healthier tissue product.

5.4 Future Directives

The assessment of the toxicity of drugs is a quintessential issue that has associated economical implications. With this novel technique, pharmaceutical companies can more quickly

identify drug failure due to nephrotoxicity. There is a strong drive to find alternative methods, especially using 3D tissue engineering techniques, in order to ethically, and more accurately assess the toxicity of the drug. My project has demonstrated that this novel technique for assessing the nephrotoxicity of pharmaceuticals has the ability to yield valuable information in order to eliminate toxic and ineffective substances at an early stage in the FDA approval process.

The high control utilized 1% Triton in order to demonstrate complete cell death within the tissue. However, because Triton acts as a detergent to disrupt the phospholipid bilayer, it effectively kills the cells via necrosis, rather than the apoptosis the cells experienced when exposed to cisplatin. Therefore, a future experiment design might involve the utilization of an agent that kills the cells in a more similar manner as cisplatin.

By incorporating this model into a perfusion bioreactor, we may be able to demonstrate its clinical utility for extended culture time, thereby allowing for this model to be implemented in more realistic studies of the long-term effect of cisplatin on kidney tissue. Additionally, the functionality of the kidney tissue exposed to cisplatin should also be analyzed. Because the outer medullary and sodium transporters have decreased expression in rat tissue exposed to cisplatin, the distribution of the Na^+/K^+ ATPase pump may prove to yield valuable information. Additionally, functional assays that analyze the organic anion transport, proximal tubular cell function, glucose and albumin uptake from the proximal tubule, may prove valuable for future data collection.

By establishing, perfecting, and implementing this technique into the current FDA-regulated process for the launch of a pharmaceutical onto the market, an additional step between the 2D cellular assessments and the preclinical animal experiments can be validated.

REFERENCES

Arany, I., & Safirstein, R. L. (2003). Cisplatin nephrotoxicity. *Seminars in Nephrology*, *23*(5), 460–464.

Blaauboer, B. (2002). The applicability of in vitro-derived data in hazard identification and characterization of chemicals. *Environmental Toxicology and Pharmacology*, *11*, 213–225.

Cornelison, T. L., & Reed, E. (1993a). Nephrotoxicity and hydration management for cisplatin, carboplatin, and ormaplatin. *Gynecologic Oncology*, *50*(2), 147–158.

Cornelison, T. L., & Reed, E. (1993b). Nephrotoxicity and hydration management for cisplatin, carboplatin, and ormaplatin. *Gynecologic Oncology*, *50*(2), 147–158.

Cristofori, P., Zanetti, E., Fregona, D., Piaia, A., & Trevisan, A. (2007). Renal proximal tubule segment-specific nephrotoxicity: an overview on biomarkers and histopathology. *Toxicologic Pathology*, *35*(2), 270–275.

Daley, W. P., Peters, S. B., & Larsen, M. (2008). Extracellular matrix dynamics in development and regenerative medicine. *Journal of Cell Science*, *121*(Pt 3), 255–264.

Davidson, A. (2008). Mouse kidney development. *StemBook*. doi:10.3824/stembook.1.34.1

Dos Santos, N. A. G., Carvalho Rodrigues, M. A., Martins, N. M., & Dos Santos, A. C. (2012). Cisplatin-induced nephrotoxicity and targets of nephroprotection: an update. *Archives of Toxicology*.

Fukuishi, N., & Gemba, M. (1989). Use of cultured renal epithelial cells for the study of cisplatin toxicity. *Japanese Journal of Pharmocology*, *50*, 247–249.

Guo, W. X., Ghebrehiwet, B., Weksler, B., Schweitzer, K., & Peerschke, E. I. (1999). Up-regulation of endothelial cell binding proteins/receptors for complement component C1q

by inflammatory cytokines. *The Journal of Laboratory and Clinical Medicine*, *133*(6), 541–550.

Huang, Q., Dunn, R., & Jayadev, S. (2001). Assessment of cisplatin-induced nephrotoxicity by microarray technology. *Toxicol Sci*, *63*, 196–207.

Jamieson, E. R., & Lippard, S. J. (1999). Structure, Recognition, and Processing of Cisplatin-DNA Adducts. *Chemical Reviews*, *99*(9), 2467–2498.

Kaushal, G. P., Kaushal, V., Hong, X., & Shah, S. V. (2001). Role and regulation of activation of caspases in cisplatin-induced injury to renal tubular epithelial cells. *Kidney International*, *60*(5), 1726–1736.

Kim, J., Jung, K.-J., & Park, K. M. (2010). Reactive oxygen species differently regulate renal tubular epithelial and interstitial cell proliferation after ischemia and reperfusion injury. *American Journal of Physiology. Renal Physiology*.

Kim, J., Kim, K. Y., Jang, H.-S., Yoshida, T., Tsuchiya, K., Nitta, K., Park, J.-W., et al. (2009). Role of cytosolic NADP+-dependent isocitrate dehydrogenase in ischemia-reperfusion injury in mouse kidney. *American Journal of Physiology. Renal Physiology*, *296*(3), F622–633.

Knight, A. (2007). Systemic reviews of animal experiments demonstrate poor human clinical and toxicology utility. *Altern Lab Anim*, *35*(6), 641–659.

Kosovsky, M. (2011, February 11). *3D Cell Culture Systems*. Po.

Kröning, R., Lichtenstein, A. K., & Nagami, G. T. (2000). Sulfur-containing amino acids decrease cisplatin cytotoxicity and uptake in renal tubule epithelial cell lines. *Cancer Chemotherapy and Pharmacology*, *45*(1), 43–49.

Kuhlmann, M., Burkhardt, G., & Kohler, H. (1997). Insights into potential cellular mechnisms of

cisplatin nephrotoxicity and their clinical application. *Nephrol Dial Transplant*, *12*, 2478–2480.

Lajer, H., Kristensen, M., Hansen, H. H., Nielsen, S., Frøkiaer, J., Ostergaard, L. F., Christensen, S., et al. (2005). Magnesium depletion enhances cisplatin-induced nephrotoxicity. *Cancer Chemotherapy and Pharmacology*, *56*(5), 535–542.

Leibbrandt, M. E., Wolfgang, G. H., Metz, A. L., Ozobia, A. A., & Haskins, J. R. (1995). Critical subcellular targets of cisplatin and related platinum analogs in rat renal proximal tubule cells. *Kidney International*, *48*(3), 761–770.

Leussink, B., Baelde, H., & Broekhuizen-van den Berg, T. (2003). Renal epithelial gene expression profile and bismuth-induced resistance against cisplatin nephrotoxicity. *Human Experimental Toxicology*, *22*, 535–540.

Liu, M., Chien, C.-C., Burne-Taney, M., Molls, R. R., Racusen, L. C., Colvin, R. B., & Rabb, H. (2006). A pathophysiologic role for T lymphocytes in murine acute cisplatin nephrotoxicity. *Journal of the American Society of Nephrology: JASN*, *17*(3), 765–774.

Liu, X., Van Vleet, T., & Schnellmann, R. G. (2004). The role of calpain in oncotic cell death. *Annual Review of Pharmacology and Toxicology*, *44*(1), 349–370.

Pampaloni, F., Stelzer, E. H. K., & Masotti, A. (2009). Three-dimensional tissue models for drug discovery and toxicology. *Recent Patents on Biotechnology*, *3*(2), 103–117.

Pfaller, W., & Gstraunthaler, G. (1998). Nephrotoxicty testing in vitro: What we know and what we need to know. *Environ. Health Perspect*, *106*(2), 559–569.

Principle of Measurement of LDH Cytotoxicity, TaKaRa Bio Company. Retrieved April 3, 2012, from: http://www.clontech.com/takara/US/Products/Cell_Biology/Cell_Proliferation_and_Viab

ility/EIA_Kits/LDH_Cytotoxicity_Detection_Kit?sitex=10031:22372:US.

Raju, S., Kavimani, S., Uma Maheshwara, V., & Sriramulu Reddy, K. (2011). Nephrotoxicants and nephrotoxicity testing: An outline of in vitro alternatives. *Journal of Pharmaceutical Sciences*, *3*(3), 1110–1116.

Ramesh, G., & Reeves, W. B. (2002). TNF-alpha mediates chemokine and cytokine expression and renal injury in cisplatin nephrotoxicity. *The Journal of Clinical Investigation*, *110*(6),

Riedemann, L., Lanvers, C., Deuster, D., Peters, U., Boos, J., Jürgens, H., & am Zehnhoff-Dinnesen, A. (2008). Megalin genetic polymorphisms and individual sensitivity to the ototoxic effect of cisplatin. *The Pharmacogenomics Journal*, *8*(1), 23–28.

Rodríguez-García, M. E., Quiroga, A. G., Castro, J., Ortiz, A., Aller, P., & Mata, F. (2009). Inhibition of p38-MAPK potentiates cisplatin-induced apoptosis via GSH depletion and increases intracellular drug accumulation in growth-arrested kidney tubular epithelial cells. *Toxicological Sciences: An Official Journal of the Society of Toxicology*, *111*(2),

Ross, M., Romrell, L., & Kaye, G. (1995). *Histology: A text and atlas* (3rd ed.). Williams & Wilkins.

Rovetta, F., Stacchiotti, A., Consiglio, A., Cadei, M., Grigolato, P. G., Lavazza, A., Rezzani, R., et al. (2012). ER signaling regulation drives the switch between autophagy and apoptosis in NRK-52E cells exposed to cisplatin. *Experimental Cell Research*, *318*(3), 238–250.

Russell, W., & Burch, R. (1992). *The Principles of Humane Experimental Technique*. London: Methuen & Co. Ltd.

Sadzuka, Y., Iwazaki, A., Miyagishima, A., Nozawa, Y., & Hirota, S. (1994). Effect of drugs in intrecellular concentration of adriamycin in Ehrlich ascites carcinoma. *Drug Deliv. Syst.*, *9*, 161–166.

Sands, J., & Verlander, J. (1997). Functional Anatomy of the Kidney. *Comprehensive Toxicology* (2nd ed., Vol. 7). New York, NY: Pergaman Press.

Schmitz, C., Hilpert, J., Jacobsen, C., Boensch, C., Christensen, E. I., Luft, F. C., & Willnow, T. E. (2002). Megalin deficiency offers protection from renal aminoglycoside accumulation. *The Journal of Biological Chemistry*, *277*(1), 618–622. doi:10.1074/jbc.M109959200

Schmoldt, A., Benthe, H. F., & Haberland, G. (1975). Digitoxin metabolism by rat liver microsomes. *Biochemical Pharmacology*, *24*(17), 1639–1641.

Servais, H., Ortiz, A., Devuyst, O., Denamur, S., Tulkens, P. M., & Mingeot-Leclercq, M.-P. (2008). Renal cell apoptosis induced by nephrotoxic drugs: cellular and molecular mechanisms and potential approaches to modulation. *Apoptosis: An International Journal on Programmed Cell Death*, *13*(1), 11–32.

Shimazu, K., Toda, S., Miyazono, M., Sakemi, T., & Sugihara, H. (2001). Morphogenesis of MDCK cells in a collagen gel matrix culture under stromal adipocyte-epithelial cell interaction. *Kidney International*, *60*(2), 568–578.

Sirichanchuen, B., Pengsuparp, T., & Chanvorachote, P. (2012). Long-term cisplatin exposure impairs autography and causes cisplatin resistance in human lung cancer cells. *Mol Chell Biochem*, *364*, 11–18.

Stanfield, C. L., Germann, W. J., Niles, M. J., & Cannon, J. G. (2008). *Principles of human physiology*. San Francisco: Pearson/Benjamin Cummings.

Subramanian, B., Rudym, D., Cannizzaro, C., Perrone, R., Zhou, J., & Kaplan, D. L. (2010). Tissue-engineered three-dimensional in vitro models for normal and diseased kidney. *Tissue Engineering. Part A*, *16*(9), 2821–2831.

Thompson, K., Afshari, C., & Amin, R. (n.d.). Identification of platform-independent gene

expression markers of cisplatin nephrotoxicity.

Tsuruya, K., Ninomiya, T., Tokumoto, M., Hirakawa, M., Masutani, K., Taniguchi, M., Fukuda, K., et al. (2003). Direct involvement of the receptor-mediated apoptotic pathways in cisplatin-induced renal tubular cell death. *Kidney International*, *63*(1), 72–82.

USDA Health and Human Services. (2004, March). Challenges and Opportunities Report. Food and Drug Administration. Retrieved from http://www.fda.gov/ScienceResearch/SpecialTopics/CriticalPathInitiative/CriticalPathOpportunitiesReports/ucm077262.htm

Villegas, G., Lange-Sperandio, B., & Tufro, A. (2005). Autocrine and paracrine functions of vascular endothelial growth factor (VEGF) in renal tubular epithelial cells. *Kidney International*, *67*(2), 449–457.

Wilkinson, J. (2009, April 1). *Tissue engineering: A new dimension to animal replacement*. Presented at the Biotechnology and biological sciences research council, Central London.

Yamate, J., Sato, K., Ide, M., Nakanishi, M., Kuwamura, M., Sakuma, S., & Nakatsuji, S. (2002). Participation of different macrophage populations and myofibroblastic cells in chronically developed renal interstitial fibrosis after cisplatin-induced renal injury in rats. *Veterinary Pathology*, *39*(3), 322–333.

Yao, X., Panichpisal, K., Neil Kurtzman, & Nugent, N. (2007). Cisplatin Nephrotoxicity: A Review. *The American Journal of the Medical Sciences*, *334*(2), 115–124.

Zhang, Z., Pascuet, E., Hueber, P.-A., Chu, L., Bichet, D. G., Lee, T.-C., Threadgill, D. W., et al. (2010). Targeted inactivation of EGF receptor inhibits renal collecting duct development and function. *Journal of the American Society of Nephrology: JASN*, *21*(4), 573–578.